ORIGINAL RESEARCH

Starch-based biocomposite membrane reinforced by orange bagasse cellulose nanofibers extracted from ionic liquid treatment

Diego B. Menezes · Fernando M. Diz · Luiz F. Romanholo Ferreira ·
Yendry Corrales · José R. V. Baudrit · Luiz P. Costa · Maria L. Hernández-Macedo

Abstract Agricultural crop residues are known to be a renewable source of value-added products, and their application as a bio-based production chain type in the circular bioeconomy system is considered efficient in minimizing environmental problems. Value-added products, such as cellulose nanofibers (CNFs) from lignocellulose in agriculture residues, have been widely applied in the production of membranes that have desirable physicochemical characteristics. In this work, orange bagasse residue was used to obtain cellulose nanofiber and then applied to starch membranes as a mechanical reinforcement. The 1-methylimidazolium ionic liquid was used as biomass treatment for cellulose nanofiber isolation, and then two starch membranes were prepared with 5% (v/v) of cellulose nanofiber solution at 70 °C and 90 °C by the casting method. The cellulose nanofibers and membranes were characterized by scanning electron microscopy, fourier transform infrared spectroscopy, thermogravimetric analysis, and X-ray diffraction. Thickness and tensile tests were applied to the membranes. Cellulose nanofibers less than 100 nm in diameter were obtained by the

D. B. Menezes · M. L. Hernández-Macedo (✉)
Graduate Program in Industrial Biotechnology, Tiradentes University, Aracaju, SE 49032-490, Brazil
e-mail: lucyherma@gmail.com

F. M. Diz
Pontifical Catholic University of Rio Grande do Sul – PUCRS, Porto Alegre, RS 90619-900, Brazil

L. F. Romanholo Ferreira · M. L. Hernández-Macedo
Institute of Technology and Research, Tiradentes University, Aracaju, SE 49032-490, Brazil

Y. Corrales · J. R. V. Baudrit
National High Tech Center, Lanotec,
10221001021 Pavas, San José, Costa Rica

L. P. Costa
Graduate Program in Science and Technology for Amazon Resources, Institute of Exact Sciences and Technology, Federal University of Amazonas, Itacoatiara, AM 69103-128, Brazil

1-methylimidazolium treatment, and the characterization analyses showed that the CNFs were incorporated into the membranes, which improved their mechanical resistance and thermal degradation capacity. However, membrane 1, which was prepared at 70 °C, showed a particularly significant gain in tensile strength.

Introduction

Lignocellulose derived from industrial and agricultural waste is a renewable material with a potential conversion to several high value compounds. This material can be successfully applied to bio-based production chain types in the circular bioeconomy system, in which reusing and recycling biomass waste is considered to minimize environmental problems related to its accumulation. The bio-waste from agricultural crops and the forestry industry is considerable at the global level, amounting to several gigatons per year. The polymeric constitution of cellulose, hemicellulose, and lignin in their fibers has shown promise as feedstock in several industrial sectors (Oliveira et al. 2016; Pleissner et al. 2016; Menezes et al. 2017; Pires et al. 2018; Meneses et al. 2020). These biopolymers are widely used in traditional industries, such as in the manufacture of paper, chemical, fiber, films, and polymers, but they have also been explored in the production of cellulose at nanoscale (nanocellulose) for applications to new materials with good mechanical properties (Pires et al. 2018; Deepa et al. 2019). Currently, the nanocellulose market has expanded with the construction of industrial plants for commercial production in several countries, such as Canada, the United States, the United Kingdom, Norway, Sweden, Finland, and Japan, thus changing the scope of this market, which was previously restricted to a few countries (Balea et al. 2020).

Among various agricultural crops, citrus fruit, such as the orange, has generated large amounts of residue worldwide. Brazil is currently the largest exporter of orange juice, and orange production is estimated to be 16.8 million tons by 2028 or 2029. This increase will also reflect the amount of bagasse orange waste available as a renewable source of value-added products that have several commercial applications, such as nanocellulose. However, to obtain nanocellulose from any lignocellulosic residue, it is necessary to depolymerize the cell walls by chemical, chemical–mechanical, or even biological treatments (Bhatia et al. 2020). The choice of the raw material and the treatment type depend on the application intended for the cellulose polymer because depolymerization techniques change the size, order, and structure of the cellulose fiber chain, thus changing its morphology (Kakroodi et al. 2014). The depolymerization of cellulose fiber leads to the formation of cellulose nanofibers (CNFs) and cellulose nanocrystals (CNCs). CNFs consist of aggregates of long thread-like bundles of cellulose chain molecules with long, flexible, and entangled, whereas CNCs are rod-like or needle-like particles with high purity, high crystallinity, and high specific surface areas (Khalil et al. 2014; Golmohammadi et al. 2017; Trache et al. 2017; Deepa et al. 2019).

The conventional procedures used in the production of CNFs are mechanical and/or acid hydrolysis or alkali pretreatment, which allow for obtaining flexible nanofibers 5–100 nm in diameter and 500–2000 nm in length (Klemm et al. 2011; Khalil et al. 2012; Brinchi et al. 2013; Deepa et al. 2015; Tan et al. 2015; Phanthong et al. 2018). Among lignocellulosic residues, peel and bagasse orange are promising sources of cellulose nanofibers (Tsukamoto et al. 2013; Hideno et al. 2014; Mariño et al. 2018), which has led to patents (Tasic et al. 2013) and companies that manufacture sustainable fabrics from citrus juice byproducts (Santanocito and Arena 2019). However, the process used to obtain cellulose nanofibers is still conventional (i.e., mechanical, acid, and alkaline) and contrary to the circular bioeconomy.

In this context, ionic liquids (LI) are an alternative to lignocellulose treatment because of their high specificity for the dissolution of amorphous cellulose and their potential for recycling and reusing after the extraction process, thus minimizing negative effects on the environment. In addition, LIs are considered green solvents because they contribute characteristics such as low vapor pressure, high thermal and chemical stability, non-flammability, and the possibility of modulation (Yoo et al. 2017; Halder et al. 2019;

Abushammala and Mao 2020). In addition, ionic liquids composed of imidazole salts, have a short cationic chain and, consequently, less steric impedance and greater diffusion capacity, thus increasing the efficiency of the depolymerization process (Zhang et al. 2013; Meenatchi et al. 2017).

CNFs obtained from renewable materials and ecofriendly processes are relevant because they are used as mechanical reinforcement materials in fields such as electronics, food, textiles, medicine, pharmaceuticals, biosensors, and polymers (Dufresne 2017; Rajinipriya et al. 2018; Joshi and Adak 2019; Quesada-González et al. 2019; Lopez-Polo et al. 2020; Wang et al. 2020). In the field of polymer science, biodegradable membranes reinforced with CNFs appear to be a promising alternative in the packaging industry. The use of non-renewable resources is limited because of the harmful effects of synthetic polymers on environmental pollution (Abral et al. 2020; Hai et al. 2020).

Cellulose nanofibers have been used in composites to reinforce water-soluble biopolymers such as starch (Balakrishnan et al. 2017; Yousefhashemi et al. 2019), cellulose acetate (Battirola et al. 2017) and gelatin (Liu et al. 2018; Seo et al. 2020). The materials resulting from this incorporation have been shown to improve the performance of mechanics, porosity, hydrophilicity, and biocompatibility compared with natural matrix polymers. In this context, this paper presents a proposal to synthesize nanocomposites associated with CNFs previously extracted through hydrolysis using ionic liquids and to test their efficiency in mechanical reinforcement.

In this work, the effects of CNF incorporation on starch membrane performance were examined. The study focused on the use of ionic liquids to obtain CNFs from orange bagasse, a waste produced in large quantities, which is explored as a renewable source to obtain value-added products.

Materials and methods

Materials

The raw material used in this work was obtained from orange bagasse (*Citrus sinensis*) supplied by the Maratá Sucos do Nordeste Ltda factory, which is located in the municipality of Estância/Sergipe.

Orange peel was previously dried at 90 °C for 24 h and then ground in a domestic multiprocessor to obtain 32-mesh granulometry. The 1-methylimidazolium ionic liquid was provided by Sigma-Aldrich (USA). All other chemicals used in this experiment were of analytical grade, and the solutions were prepared with deionized water.

Biomass treatment and cellulose nanofiber extraction

Orange residue at 32-mesh granulometry was treated with 1-methylimidazolium ionic liquid at the ratio of 1:10 m/v (residue/IL) and vigorously stirred (1000 rpm) at 90 °C for 2 h. After the treatment, the resulting suspension was subjected to centrifugation at $10000 \times g$ for 10 min. Subsequently, the precipitated material underwent a dialysis process in water to remove excess LI (pH between 6 and 7). The suspension was then sonicated for 5 min and stored at 8 °C after the addition of five drops of chloroform (Dong et al. 1998; Pelissari et al. 2014). The residues generated during the biomass treatment and the obtained CNFs (liquid and solid residues) were recovered through the rotary evaporation and reused in other research work.

Preparation of starch membrane reinforced with cellulose nanofibers

Two membranes were prepared using the solvent casting method. The membranes (1 and 2) were prepared by mixing soluble corn starch (1.2 g) with 0.8 g of glycerol and 40 mL of deionized water, which was then subjected to agitation at 1200 rpm for 2 h under a heating bath. The temperatures of the heating bath were 70 °C to prepare membrane 1 and 90 °C to prepare membrane 2. In the last 10 min of both shaking membrane base solutions, 5% (v/v) of cellulose nanofiber solution (11.33 mg/mL) was incorporated.

The nanocomposite solutions were subjected to ultrasound treatment to remove bubbles formed during heating and stirring (Potency: 42 kHz for 10 min). Then 20 mL of the membrane-forming mixture was added to PE plates (polyethylene) and air dried for approximately 48 h at 40 °C. Next, the membranes (nanocomposites) were kept in a desiccator to control their humidity before being characterized (Silva et al.

2015). A membrane without the addition of cellulose nanofibers was used as a control.

Characterization of cellulose nanofibers and nanocomposites

Electron microscopy of cellulose nanofibers and nanocomposites

Cellulose nanofibers and nanocomposites were evaluated by scanning electron microscopy (*Shimadzu Super Scan SSX550 model*). The membranes without CNFs and nanocomposites were previously lyophilized for 24 h at −55 °C using Liotop's L101 equipment and later metalized with a thin layer of gold by sputtering at an exposure time of 2 min. The accelerating voltage was 15 kV.

In addition to the SEM, the cellulose nanofibers were evaluated by atomic force microscopy performed on a multimodal AFM (DI, Veeco, Instrumentation Group). Silicon nitride cantilevers (SiNi, silicon nitride) were used in contact mode at a resonance frequency of 1 kHz, a spring constant between 0.15 and 0.30 N, and a peak radius of 100 nm. The samples were prepared by dilution at 0.5 gL^{-1} in ultrapure water (Milli-Q) and placed on a mica substrate and dried at room temperature. The CNF image analysis was performed using Nanoscope Software 7.3.

Fourier transform infrared spectroscopy (FTIR)

The *in-nature* orange bagasse residue, as well as the CNFs and the nanocomposite, were submitted to FTIR analysis in ATR mode using Fourier transform infrared spectrometer equipment (FTIR—Nicolet IS10, Thermo Scientific). The spectrum of each sample was analyzed at a range of 4000–500 cm^{-1}; 32 scans per each sample were taken.

Thermogravimetric analysis (TGA)

Thermogravimetric analyses of the samples (8 mg) were performed in a thermal analyzer (TA Q500, TA Company) using a platinum crucible, a nitrogen flow of 20 mL min^{-1} at a heating rate of 10 °C min^{-1} in the temperature range of 25–1000 °C (Chen et al. 2020).

X-ray diffraction (XRD)

The crystallinity of the samples was analyzed using the Shimadzu X-ray diffractometer, model XRD-6000 at CuKα radiation, λ = 1.5406 Å, and an angular pitch of 0.05°. The samples were analyzed in the angular range of 5°–40° (Bragg angle = 2θ) at a temperature of 23 ± 2 °C and an exposure time of 1 s per angle (Ninomiya et al. 2018; Segal et al. 1959). The crystallinity of the samples was determined by the following equation:

$$CrI = \frac{I_{002} - I_{am}}{I_{002}} \times 100$$

where I_{002} and I_{am} are the maximum intensity of the (002) lattice diffraction and the minimum intensity between the (101) and (002) lattice planes, respectively.

Nanocomposite thickness (T) and Tensile test

The thickness of the nanocomposites at 60% RH and 25 °C was measured using a flat-tip Mitutoyo digital micrometer (1 μm resolution) by 3-point random measurements.

The tensile tests were performed in a universal test machine (Discovery HR-3/Hybrid Rheometer, TA Company) with a maximum load of 20 N and a testing speed of 12.5 mm min^{-1} at 25 °C, according to ASTM D-882. Traction tests were performed on three specimens (15 mm × 2 mm) of each sample (Silva et al. 2015).

Results and discussion

Morphological analysis of cellulose nanofibers

The morphology of the cellulose nanofibers obtained from the 1-methylimidazolium treatment was evaluated by SEM image, as shown in Fig. 1. The lowest magnification image of the cellulose nanofibers is shown in Fig. 1a. SEM image with 30,000 magnification shows a nanofiber tangle formed from the defibrillation process of the sample (Fig. 1b). The CNFs extracted by the treatment with LI is shown in Fig. 1c, which exhibits a network of nanofibers that are arranged in a random manner at diameters not exceeding 100 nm. A similar morphology was
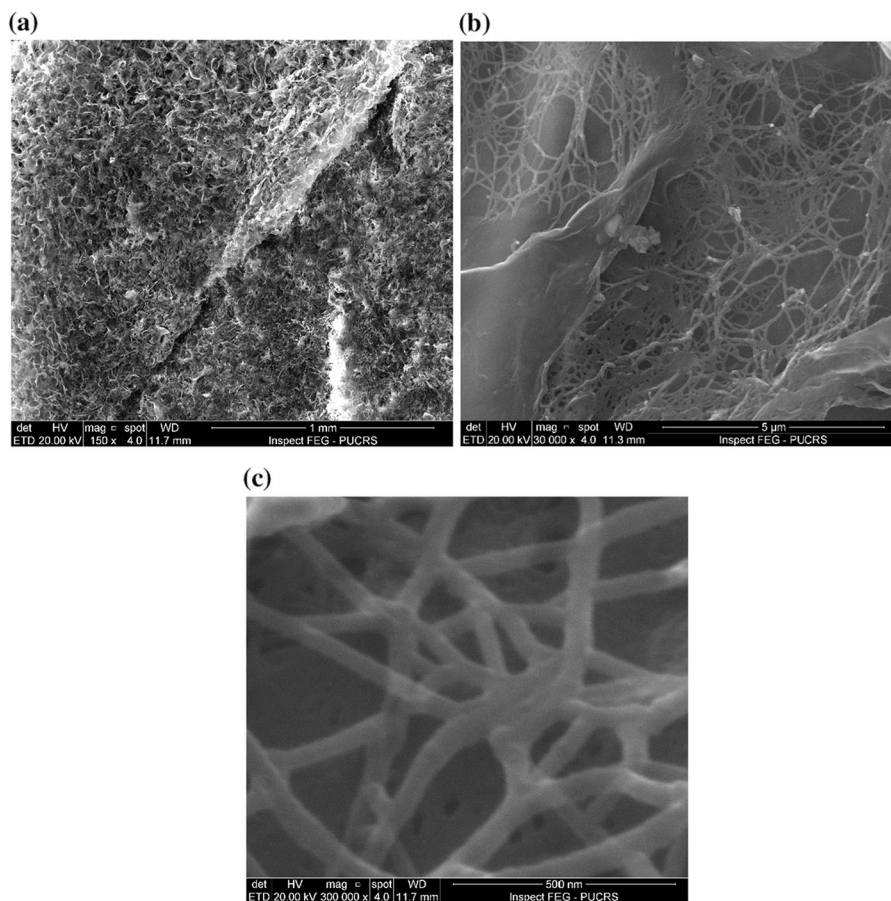
Fig. 1 Scanning electron microscopy of cellulose nanofibers extracted from ionic liquid 1- methylimidazolium treatment. The micrographs were captured in increases of 150 × (**a**), 30,000 × (**b**), and 300,000 × (**c**)

observed in the nanofibers obtained by treating with ionic liquids in other residues (Pereira et al. 2020; Moyer et al. 2018; Ninomiya et al. 2018). This result indicated that the use of ionic liquids is an alternative method for obtaining CNF. In addition to scanning electron microscopy, the nanofibers were evaluated by atomic force microscopy (Fig. 2). Thus, it was possible to complement the results of the SEM, confirming that the nanofibers were within the nanometric scale at an average below 100 nm, which was necessary for the synthesis of the proposed nanobiocomposite.

Thermogravimetric analysis (TGA)

The thermogravimetric analysis performed using natural orange residue, CNFs, and the membrane samples (Fig. 3) revealed four stages of degradation

(1°—25–120 °C [approximately]; 2°—120–300 °C; 3°—300–375 °C; and 4°—375–670 °C).

The first stage was related to the loss of uncontaminated water by dehydration, which was not evident because of the adjustment of the isothermal parameter in the equipment used, which counted the mass loss from the pre-set 40 °C. In the second stage, it was possible to observe the loss of water that was molecularly bound to the structure of the studied samples, as well as the degradation of associated compounds that are on the surface of each material.

The highest percentage of mass loss occurred between the second and third stages, which confirmed the higher concentration of easily degraded polymers and associated compounds (i.e., starch and cellulose). In particular, in the third stage, it was possible to identify the region of the mass loss of cellulose and carbonic chains at the temperature of 375 °C. In
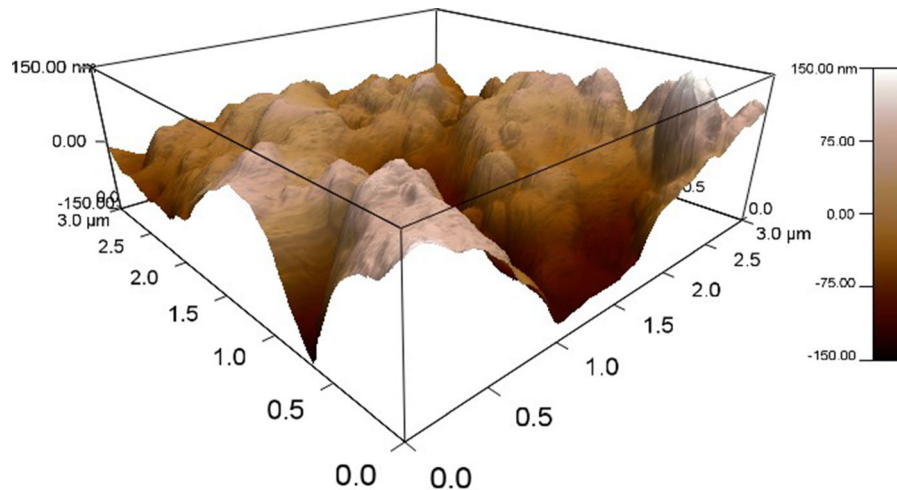
Fig. 2 Three-dimensional graph obtained by the AFM analysis of cellulose nanofibers extracted from orange bagasse using 1-methylimidazolium
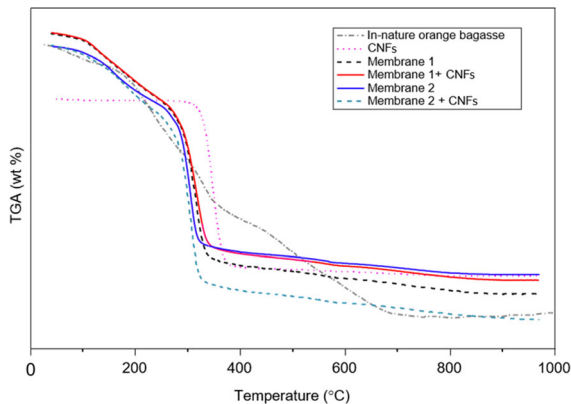

Fig. 3 Thermogravimetric analysis of the natural orange bagasse samples, the cellulose nanofibers (CNFs) extracted using 1-methylimidazolium, and membranes with and without the addition of CNFs

addition, in observing the pattern of events, it was identified that the sample of the natural residue exhibited a different pattern of the number of mass loss events. This was evident when it presented a very expressive fourth event between 375 and 670 °C, which was characterized by the degradation of stronger components, such as lignin, which were still associated in the sample.

In general, the technique was aimed to confirm the efficiency of the chemical treatment in removing the other lignocellulosic components (i.e., hemicellulose and lignin), either entirely or partially. This was evident in the thermal behavior of the CNF sample

obtained after the extraction process, which showed a single degradation event between 300 and 375 °C, characterized by cellulose degradation, as reported by Meenatchi et al. (2017). At this point, the cellulose nanofibers showed degradation events between 290 and 375 °C (Orrabalis et al. 2019), as shown in Fig. 3. Therefore, no significant difference was observed between the thermal degradation of cellulose results in the literature and the TGA analysis of CNFs. Thus, the thermal degradation of the samples shown in Fig. 3 suggests that CNFs were released during the depolymerization of the lignocellulosic residue.

Fourier transform infrared (FTIR) analysis

The FTIR analysis allowed the identification of the main chemical groups in the evaluated samples (i.e., natural orange residue, CNFs, and membranes) as well as variations in their molecular composition and the presence of CNF in the starch matrix (Fig. 4).

The FTIR region between 3000 and 3600 cm^{-1} corresponded to the hydroxyl group vibration elongation (O–H), which has been associated with the presence of water in analyzed residues (Liu et al. 2018). Peaks in the region of 2900 cm^{-1} were attributed to the symmetrical and asymmetrical overlap of C–H and the elongation of the vibration of the aliphatic chain in the spectrum, which may be attributed to the cellulose in the sample (Asad et al.

Fig. 4 FTIR spectra of cellulose nanofibers (CNFs); starch, Membrane 1 (control); Membrane 1 + CNFs; Membrane 2 (control); Membrane 2 + CNFs
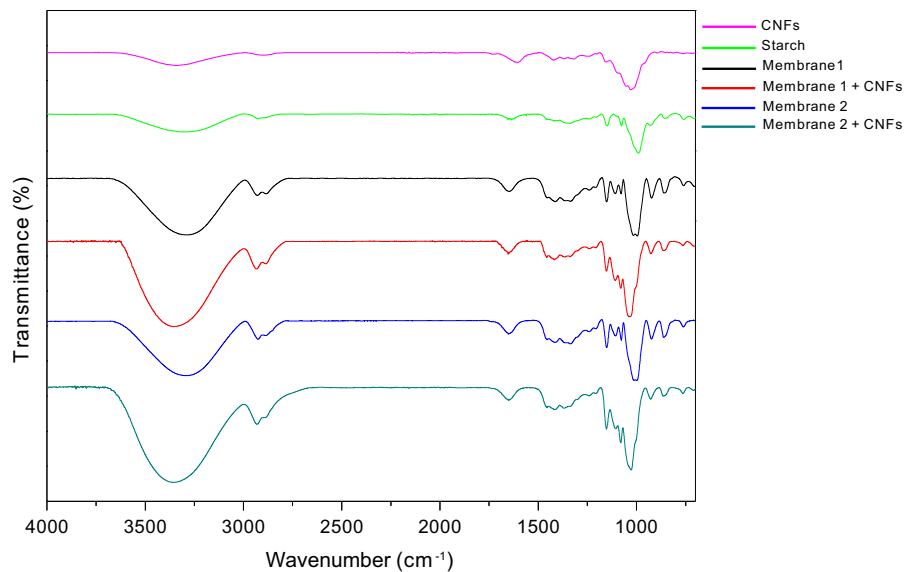
2018; Liu et al. 2018). Thus, it was observed that in the membranes with cellulose nanofibers, the bonds had greater intensity, suggesting the stability of the nanofibers in the membrane matrix.

The bands identified between 1645 and 1632 cm^{-1} were attributed to the elongated vibration of absorbed water (H–O–H) by carbohydrates with an increasing peak due to less crystallinity (Lee et al. 2015; Rambabu et al. 2016). These bands were also observed in membranes 1 and 2, suggesting a decrease in crystallinity due to water absorption by the starch.

The bands observed near 1428 cm^{-1} were related to the flexion of C–H present in the carbon chains (Wang et al. 2017), which were related to the concentration of the cellulose chains in the samples. According to Benini et al. (2018), the region close to 1000 cm^{-1} is associated with the narrowing of CO bonds, which form bands corresponding to the spectra of membranes associated with CNFs. These bands were more evident in membranes 1 and 2 associated with CNFs, suggesting its incorporation during the nanocomposite preparation. In addition, this region was characterized by vibrations related to β-glycosidic bonds. In this case, peaks were observed in the spectra of the membrane samples, especially those with incorporated nanofibers. Their composition included a higher concentration of carbohydrates with this type of chemical bond, which also supported the incorporation of cellulose nanofibers in the formulated membranes.

X-ray diffraction analysis of CNFs and starch membranes

The results of the XRD showed differences between the standard membranes and the membranes with the addition of CNFs, which were evidenced by the intensity of the peaks (Fig. 5). Crystaline peaks near the angles of 14.8°, 16.5°, 22.2°, and 35° corresponded to planes of crystalline cellulose type I. Despite the low intensity of the peak at 35° in relation to the other peaks, it was the most evident in the diffractograms of the membranes associated with cellulose nanofiber (Zain et al. 2014; Meenatchi et al. 2017; Sofla et al. 2016; Mariño et al. 2018). Authors as Kalita et al. (2015), Nascimento et al. (2015) and Asad et al. (2018) also identified peaks within the same regions that were reported in this study, which supports the incorporation of nanomaterial in the polymeric membrane matrix. The peak of 22.2°, which is highlighted in the literature as the reference peak of cellulose nanofibers, was observed in all diffractograms, but at different intensities, thus, indicating the presence of CNFs incorporated in the matrix of the membranes (Miranda et al. 2015; Theivasanthi et al. 2018). This was observed in the difference between the membranes, where those with CNFs in their composition presented higher intensity in all peaks corresponding to the crystallinity of the cellulose.

Moreover, it was identified that the peaks presented a higher base thickness, which characterizes

Fig. 5 Diffractogram (XRD) of the cellulose nanofibers (CNFs) extracted using 1-methylimidazolium and membranes with and without the addition of CNFs
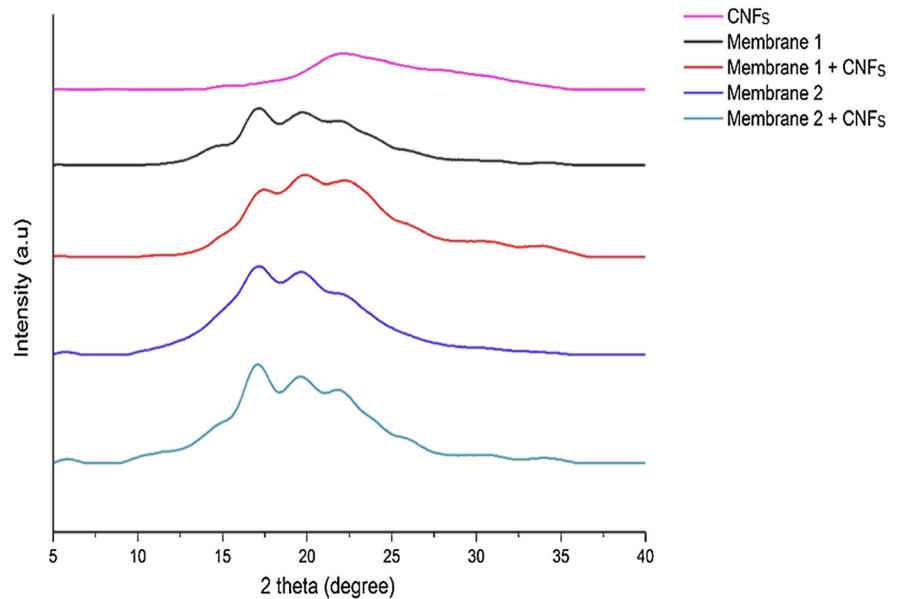
polymorphic material as well as the alternating crystalline and semicrystalline domains of cellulose and starch (Frost et al. 2009; Li et al. 2015).

After identifying the peaks that corresponded to cellulose, the crystallinity index (CI) of the membranes was calculated to highlight increases in the crystallinity of the composite, which were associated with the addition of CNFs in the formulation. The membranes with CNFs showed a CI with values of 16.77% in membrane 1 + CNFs and an IC of 3.13% in membrane 2 + CNFs. In contrast, the membranes of the control group had an IC of 6.89% (membrane 1), whereas a negative IC (-18.51%) was identified in membrane 2 (Table S1).

In general, the low results of the IC of the membranes compared with CNFs (75.23%) were directly related to the low concentration of CNFs in the starch, the major fraction of the matrix, which exhibited a semicrystalline profile (Thiré et al. 2005; Cheng et al. 2017; Pozo et al. 2018). In addition, the negative or null value of CI in membrane 2 (Table S1) was due to the temperature used in the solubilization of the components (90 °C). Temperatures between 90 and 180 °C lead to a change in the molecular organization of the starch, which promote a transition from semicrystalline to amorphous, forming a type of starch known as thermoplastic starch (Blanshard 1987; Corradini et al. 2007; Zhang et al. 2014; Osorio et al. 2019). Therefore, the increase in the amorphous

portion of the starch in relation to the crystalline support the result found in membrane 2.

Scanning electron microscopy (SEM) of membranes

According to the results observed in the micrographs of the membranes, it was possible to identify some differences between those that had the starch + glycerol matrix and those that, in addition to these components, had the addition of cellulose nanofibers.

Figure 6 shows the membranes with and without the cellulose nanofiber addition. In Fig. 6a, membrane 1 without CNFs, the surface presents wrinkles and a less homogeneous appearance, while in membrane 2 (Fig. 6c) these irregularities present in the form of depressions. These results could be associated with the preparation methodology and the temperature differences used in their production. In membrane 1, the temperature was 70 °C; in membrane 2, the temperature was 90 °C. Thus, the temperature difference directly influenced the solubilization of the suspension starch (Faria et al. 2017; Souza et al. 2015).

Figure 6b, 6d show membranes with the addition of CNFs, which appeared similar to the others with the addition of a greater concentration of surface irregularities attached to the networks formed by the fibers,
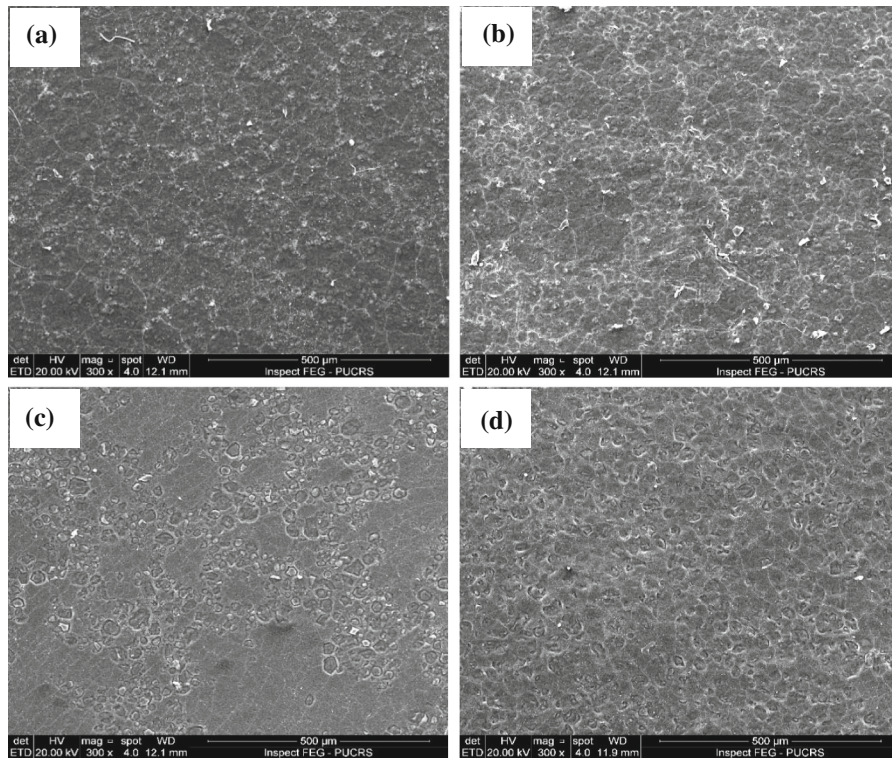
Fig. 6 SEM of the membranes produced using 1.2 g of starch, 0.8 g of plasticizer, and 40 mL of H_2O through heating in a water bath at 70 °C (Membrane 1 (**a**); Membrane 1 + CNFs (**b**)) and 90 °C (Membrane 2 (**c**); Membrane 2 + CNFs (**d**))

which promoted the formation of internal pores that caused irregularities in the surface.

Thickness and tensile testing

As shown in Table 1, the values of the thickness of the membranes synthesized were similar with low standard deviations, which indicated that the tensile tests revealed little relative interference in structural differences, which supported the validation of the data in this study.

Figure 7 a, b show membranes 1 and 2, for which different temperatures were used in preparing the suspension. Therefore, the tensile behavior of the membranes was observed without the addition of cellulose. The axial strengths of membranes 1 and 2 were 0.4 and 0.45 (N/mm^2), respectively. The lower GPa represents the modulus of elasticity in membranes 1 and 2, the durations of which were less during the events of elastic and plastic deformation, at 220 s and 170 s, respectively.

As shown in Figs. 7c and 6d (membranes 1 and 2, respectively, with CNF addition), an increase in axial

Table 1 Thickness, width, and length tests of membranes with and without the addition of cellulose nanofibers (CNFs).

	Thickness	Width	Length
Membrane 1	0.18 mm ± 0.01	5.65 mm ± 0.05	14.80 mm ± 0.14
Membrane 2	0.17 mm ± 0.02	5.49 mm ± 0.21	14.94 mm ± 0.38
Membrane 1 + CNF	0.17 mm ± 0.01	5.44 mm ± 0.10	14.81 mm ± 0.36
Membrane 2 + CNF	0.17 mm ± 0.01	5.55 mm ± 0.12	15.13 mm ± 0.16

The measurements of each membrane were taken in triplicate
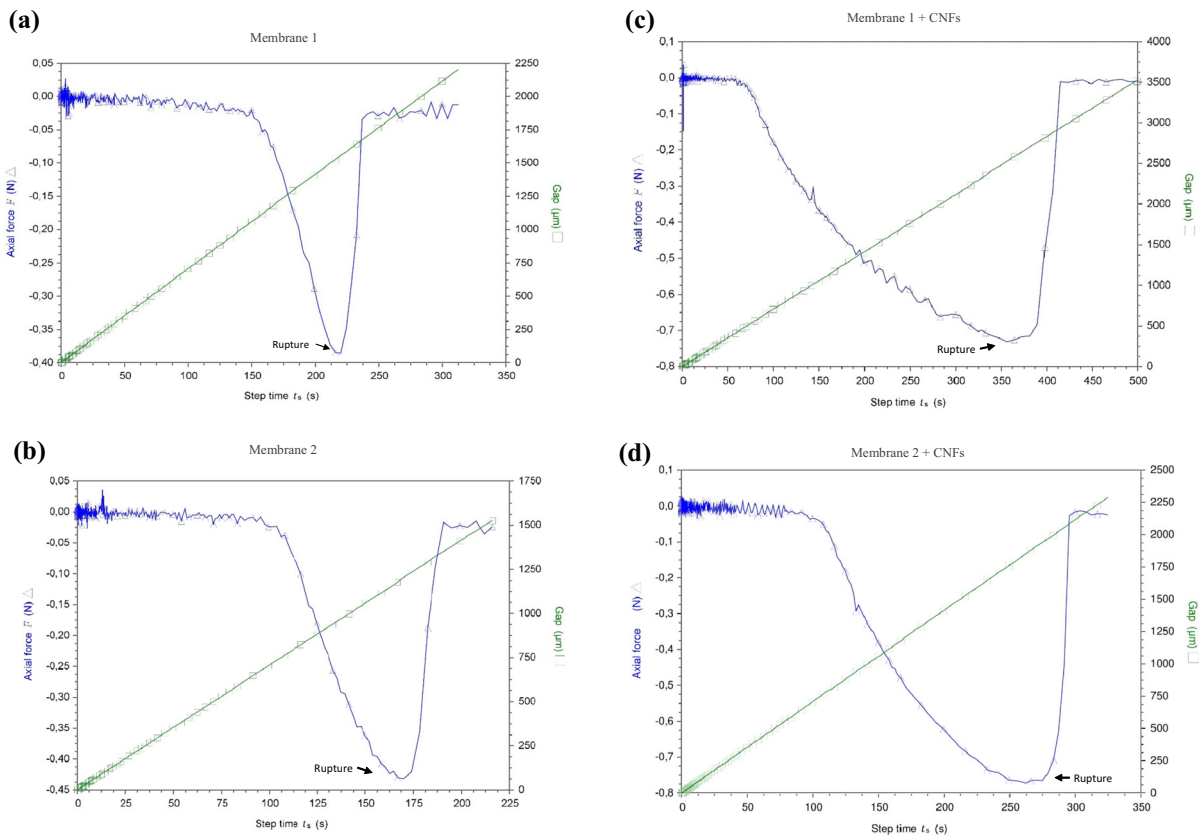
(a)

(c)

(b)

(d)

Fig. 7 Graphs of the tensile test of the membranes. (a) Membrane 1; (b) Membrane 2; (c) Membrane 1 + cellulose nanofibers (CNFs); (d) Membrane 2 + cellulose nanofibers (CNFs)

force (F) was observed at 0.74 and 0.78 N (N/mm^2), which corresponded to an increase in strength in relation to the control membrane (without CNFs): 85% in membrane 1, and 73.33% in membrane 2. In addition, an increase in the modulus of elasticity (GPa) was also identified. In membrane 1, the GPa value increased from 2125 to 3500 μm with the addition of CNFs, resulting in an overall increase of 64.7%. In membrane 2, the GPa value increased from 1562.5 to 2312.5 μm with the addition of CNFs, resulting in an overall increase of 48%. The highest values in the tensile test observed in the membranes with CNF addition may be attributed to the improved dispersion in the starch matrix and the compatibility and formation of hydrogen bonds between the starch and CNFs (Agustin et al. 2014; Fan et al. 2016). These physicochemical characteristics can be influenced by the temperature used in the membranes prepared, which explains the high value in membrane 1 with CNFs. According to the literature, the larger the module, the

greater the mechanical strength and the resistance to elastic deformation (Berglund et al. 2016; Nechyporchuk et al. 2018). A considerable increase was observed in the limit and time of elastic and plastic deformation at 350 s and 275 s, respectively, in membranes 1 and 2, as well as an increase of cellulose, which corresponded to increases of 59.09% and 61.76% in deformation time, which indicated that more work was needed to promote the rupture of the membranes.

Conclusion

Cellulose nanofibers obtained from orange peel treated with 1-methylimidazolium was used to reinforce starch membrane. The ionic liquid was effective in lignocellulosic matter depolymerization and the consequent release of cellulose nanofibers. The SEM and AFM analysis confirmed CNFs obtention at a

diameter not greater than 100 nm, which indicated their potential application in the synthesis of nanocomposites for different purposes. Cellulose nanofibers were incorporated into starch polymer matrices to form a nanocomposite with improved mechanical properties. The membranes with the addition of cellulose nanofibers showed considerable increases in the strength and deformation time parameters. However, membrane 1, prepared at 70 °C, showed the most significant gain in tensile strength (11.7% higher than membrane 2), probably due to the better dispersion of the starch matrix at this temperature in association with the incorporation of cellulose nanofibers. The CNF extraction, as well as the prepared composites, indicated the potential for cleaner alternative processes for obtaining new materials, thus adding value to orange bagasse, a common waste in the agroindustry.

Declaration

Conflict of interest The authors declare that they have no conflict of interest.

References

Abral H, Ariksa J, Mahardika M, Handayani D, Aminah I, Sandrawati N, Sapuan SM, Ilyas RA (2020) Effect of ultrasonication duration of polyvinyl alcohol (PVA) gel on characterizations of PVA film. J Mater Res Technol 9(2):2477–86

Abushammala H, Mao J (2020) A review on the partial and complete dissolution and fractionation of wood and lignocelluloses using imidazolium ionic liquids. Polymers 12:195

Agustin MB, Ahmmad B, Alonzo SMM, Patriana FM (2014) Bioplastic based on starch and cellulose nanocrystals from rice straw. J Reinf Plast Compos 33:2205–2213

Asad M, Saba N, Asiri AM, Jawaid M, Indarti E, Wanrosli WD (2018) Preparation and characterization of nanocomposite films from oil palm pulp nanocellulose/poly (Vinyl alcohol) by casting method. Carbohyd Polym 191:103–111

Balakrishnan P, Gopi S, Sreekala MS, Thomas S (2017) UV resistant transparent bionanocomposite films based on potato starch/cellulose for sustainable packaging. Starch Stärke 70:1700139

Balea A, Fuente E, Monte MC, Merayo N, Campano C, Negro C, Blanco A (2020) Industrial application of nanocelluloses in papermaking: a review of challenges, technical solutions, and market perspectives. Molecules 25:526

Battirola LC, Andrade PF, Marson GV, Hubinger MD, Gonçalves MC (2017) Cellulose acetate/cellulose nanofiber membranes for whey and fruit juice microfiltration. Cellulose 24:5593–5604

Benini KCCC, Voorwald HJC, Cioffi MOH, Rezende MC, Arantes V (2018) Preparation of nanocellulose from Imperata brasiliensis grass using Taguchi method. Carbohyd Polym 192:337–346

Berglund L, Noël M, Aitomäki Y, Öman T, Oksman K (2016) Production potential of cellulose nanofibers from industrial residues: Efficiency and nanofiber characteristics. Ind Crops Prod 92:84–92

Bhatia SK, Jagtap SS, Bedekar AA, Bhatia RK, Patel AK, Pant D, Rajesh Banu J, Rao CV, Kim YG, Yang YH (2020) Recent developments in pretreatment technologies on lignocellulosic biomass: effect of key parameters, technological improvements, and challenges. Biores Technol 300:122724

Blanshard JMV (1987) Starch granule structure and function: a physicochemical approach. In: Chichester T (ed) Starch: properties and potentials, galliard, 2nd edn. Wiley, New York

Brinchi L, Cotana F, Fortunati E, Kenny JM (2013) Production of nanocrystalline cellulose from lignocellulosic biomass: technology and applications. Carbohyd Polym 94:154–169

Chen Q, Shi Y, Chen G, Cai M (2020) Enhanced mechanical and hydrophobic properties of composite cassava starch films with stearic acid modified MCC (microcrystalline cellulose)/NCC (nanocellulose) as strength agent. Int J Biol Macromol 142:846–854

Cheng G, Zhou M, Wei YJ, Cheng F, Zhu PX (2017) Comparison of mechanical reinforcement effects of cellulose nanocrystal, cellulose nanofiber, and microfibrillated cellulose in starch composites. Polym Compos 40:365–372

Corradini E, Carvalho AJF, Curvelo AAS, Agnelli JAM, Mattoso LHC (2007) Preparation and characterization of thermoplastic starch/zein blends. Mater Res 10:227–231

Deepa B, Abraham E, Cordeiro N, Mozetic M, Mathew AP, Oksman K, Faria M, Thomas S, Pothan LA (2015) Utilization of various lignocellulosic biomass for the production of nanocellulose: a comparative study. Cellulose 22:1075–1090

Deepa B, Chirayil CJ, Pothan LA, Thomas S (2019) Lignocellulose-Based nanoparticles and nanocomposites: Preparation, Properties, and Applications. In: Ariffin H, Sapuan SM, Hassan MA (eds) Lignocellulose for Future Bioeconomy. Elsevier, Amsterdam, pp 41–69

Dong XM, Revol JF, Gray DG (1998) Effect of microcrystalline of preparation condition on the formation of colloid crystals of cellulose. Cellulose 5:19–32

Dufresne A (2017) Cellulose nanomaterial reinforced polymer nanocomposites. Curr opin colloid e interface sci 29:1–8

Fan H, Ji N, Zhao M, Xiong L, Sun Q (2016) Characterization of starch films impregnated with starch nanoparticles

prepared by 2,2,6,6-tetramethylpiperidine-1-oxyl (TEMPO)-mediated oxidation. Food Chem 192:865–872

Faria PC, Martin AA, Alves NP (2017) Characterization infrared (IR) and Surface electron microscopy (SEM) of asymmetric membranes based on Poly (acrylonitrile-co-vinyl acetate). Matéria 22:1

Frost K, Kaminski D, Kirwan G, Lascaris E, Shanks R (2009) Crystallinity and structure of starch using wide angle X-ray scattering. Carbohyd Polym 78:543–548

Golmohammadi H, Morales-Narvaez E, Naghdi T, Merkoci A (2017) Nanocellulose in sensing and biosensing. Chem Mater 29:5426–5446

Hai L, Choi ES, Zhai L, Panicker PS, Kim J (2020) Green nanocomposite made with chitin and bamboo nanofibers and its mechanical, thermal and biodegradable properties for food packaging. Int J Biol Macromol 144:491–499

Halder P, Kundu S, Patel S, Setiawan A, Atkin R, Parthasarthy R, Ferreiro JP, Surapaneni A, Shah K (2019) Progress on the pre-treatment of lignocellulosic biomass employing ionic liquids. Renew Sustain Energy Rev 105:268–292

Hideno A, Kentaro A, Hiroyuki Y (2014) Preparation using pectinase and characterization of nanofibers from orange peel waste in juice factories. J Food Sci 79:1218–1224

Joshi M, Adak B (2019) Advances in nanotechnology based functional, smart and intelligent textiles: a review. reference module in materials science and materials engineering. Compr Nanosci Nanotechnol (Second Edition) 5:253–290

Kakroodi AR, Cheng S, Sain M, Asiri A (2014) Mechanical, thermal, and morphological properties of nanocomposites based on polyvinyl alcohol and cellulose nanofiber from aloe vera rind. J Nanomater 2014:1–7

Kalita E, Nath BK, Agan F, More V, Deb P (2015) Isolation and characterization of crystalline, autofluorescent, cellulose nanocrystals from saw dust wastes. Ind Crops Prod 65:550–555

Khalil AHPS, Bhat AH, Yusra AFI (2012) Green composites from sustainable cellulose nanofibrils: a review. Carbohyd Polym 87:963–979

Khalil HA, Davoudpour Y, Islam MN, Mustapha A, Sudesh K, Dungani R, Jawaid M (2014) Production and modification of nanofibrillated cellulose using various mechanical processes: a review. Carbohyd Polym 99:649–665

Klemm D, Kramer F, Moritz S, Lindstrm T, Ankerfors M, Gray D, Dorris A (2011) Nanocelluloses: a new family of nature-based materials. Angew Chem 50:5438–5466

Lee C, Dazen K, Kafle K, Moore A, Johnson DK, Park S, Kim SH (2015) Correlations of apparent cellulose crystallinity determined by XRD, NMR, IR, Raman, and SFG Methods. Adv Polym Sci. https://doi.org/10.1007/12_2015_320

Li M, Witt T, Xie F, Warren FJ, Halley PJ, Gilbert RG (2015) Biodegradation of starch films: the roles of molecular and crystalline structure. Carbohyd Polym 122:115–122

Liu R, Dai L, Si C, Zeng Z (2018) Antibacterial and hemostatic hydrogel via nanocomposite from cellulose nanofibers. Carbohyd Polym 195:63–70

Lopez-Polo J, Silva-Weiss A, Zamorano M, Osorio FA (2020) Humectability and physical properties of hydroxypropyl methylcellulose coatings with liposome-cellulose nanofibers: food application. Carbohyd Polym 231:115702

Mariño MA, Rezende CA, Tasic L (2018) A multistep mild process for preparation of nanocellulose from orange bagasse. Cellulose. https://doi.org/10.1007/s10570-018-1977-y

Meenatchi B, Renuga V, Manikandan A (2017) Cellulose dissolution and regeneration using various imidazolium based protic ionic liquids. J Mol Liq 238:582–588

Meneses DB, Vásquez GMO, Baudrit JRV, Álvarez MR, Castillo JC, Araya LCM (2020) Pretreatment methods of lignocellulosic wastes into value-added products: recent advances and possibilities. Biomass Convers Biorefinery. https://doi.org/10.1007/s13399-020-00722-0

Menezes DB, Brazil OAV, Romanholo-Ferreira LF, Polizeli MLTM, Ruzene DS, Silva DP, Costa LP, Hernández-Macedo ML (2017) Prospecting fungal ligninases using corncob lignocellulosic fractions. Cellulose 24:4355–4365

Miranda CS, Fiuza RP, Carvalho RF, José NM (2015) Effect of surface treatment on properties of bagasse piassava fiber Attalea funifera Martius. Quim Nova 38:161–165

Moyer P, Smith MD, Abdoulmoumine N, Chmely SC, Smith JC, PetridiSL LN (2018) Relationship between lignocellulosic biomass dissolution and physicochemical properties of ionic liquids composed of 3-methylimidazolium cations and carboxylate anions. Phys Chem Chem Phys 20:2508–2516

Nascimento JHO, Luz RF, Galvão FMF, Melo JDD, Oliveira FR, Ladchumananandasivam R, Zille A (2015) Extraction and characterization of cellulosic nanowhisker obtained from discarded cotton fibers. Mater Today Proc 2:1–7

Nechyporchuk O, Kolman K, Bridarolli A, Odlyha M, Bozec L, Oriola M, Bordes R (2018) On the potential of using nanocellulose for consolidation of painting canvases. Carbohyd Polym 194:161–169

Ninomiya K, Abe M, Tsukegi T, Kuroda K, Tsuge Y, Ogino C, Takahashi K (2018) Lignocellulose nanofibers prepared by ionic liquid pretreatment and subsequent mechanical nanofibrillation of bagasse powder: application to esterified bagasse/polypropylene composites. Carbohyd Polym 182:8–14

Oliveira FB, Bras J, Pimenta MTB, Curvelo AAS, Belgacem MN (2016) Production of cellulose nanocrystals from sugarcane bagasse fibers and pith. Ind Crops Prod 93:48–57

Orrabalis C, Rodríguez D, Pampillo LG, Londoño-Calderón C, Trinidad M, Martínez-García R (2019) Characterization of nanocellulose obtained from Cereus Forbesii (a South American cactus). Mater Res 22(6):e20190243. https://doi.org/10.1590/1980-5373-mr-2019-0243

Osorio J, Dreolin N, Aznar M, Nerín C, Hancock P (2019) Determination of volatile non intentionally added substances coming from a starch-based biopolymer intended for food contact by different gas chromatography-mass spectrometry approaches. J Chromatogr A 1599:215–222

Pelissari FM, Sobral PJA, Menegalli FC (2014) Isolation and characterization of cellulose nanofibers from banana peels. Cellulose 21:417–432

Pereira PHF, Ornaghi Júnior HL, Coutinho LV, Duchemin B, Cioffi MOH (2020) Obtaining cellulose nanocrystals from pineapple crown fibers by free-chlorite hydrolysis with sulfuric acid: physical, chemical and structural characterization. Cellulose 27:5745–5756

Phanthong P, Reubroycharoen P, Hao X, Xu G, Abudula A, Guan G (2018) Nanocellulose: extraction and application. Carbon Resour Convers 1:32–43

Pires JRA, Souza VGL, Fernando AL (2018) Production of nanocellulose from lignocellulosic biomass wastes: prospects and limitations. Lect Notes Electr Eng 505:719–725

Pleissner D, Qi Q, Gao C, Rivero CP, Webb C, Lin CSK, Venus J (2016) Valorization of organic residues for the production of added value chemicals: a contribution to the bio-based economy. Biochem Eng J 116:3–16

Pozo C, Rodríguez-Llamazares S, Bouza R, Barral L, Castaño J, Müller N, Restrepo I (2018) Study of the structural order of native starch granules using combined FTIR and XRD analysis. J Polym Res. https://doi.org/10.1007/s10965-018-1651-y

Quesada-González D, Stefani C, González I, Escosura-Muñiz A, Domingo N, Mutjé P, Merkoçi A (2019) Signal enhancement on gold nanoparticle-based lateral flow tests using cellulose nanofibers. Biosens Bioelectron 141:111407

Rajinipriya M, Nagalakshmaiah M, Robert M, Elkoun S (2018) Importance of agricultural and industrial waste in the field of nanocellulose and recent industrial developments of wood based nanocellulose: a review. ACS Sustain Chem Eng 6:2807–2828

Rambabu N, Panthapulakkal S, Sain M, Dalai AK (2016) Production of nanocellulose fibers from pinecone biomass: evaluation and optimization of chemical and mechanical treatment conditions on mechanical properties of nanocellulose films. Ind Crops Prod 83:746–754

Santanocito A, Arena, A (2019) Orange fiber: the company making fabrics from citrus juice waste. Publishing globalshakers. https://globalshakers.com/orange-fiber-the-company-making-fabrics-from-citrus-juice-waste/. Accessed 21 Dec 2020

Segal L, Creely J, Martin JRAE, Conrad CM (1959) An empirical method for estimating the degree of crystallinity of native cellulose using the X-ray diffractometer. Text Res J 29:786–794

Seo M, Seo M, Choi SE, Shin K, Lee JB, Yang DY, Kim JW (2020) Cellulose nanofiber-multilayered fruit peel-mimetic gelatin hydrogel microcapsules for micropackaging of bioactive ingredients. Carbohyd Polym 229:115559

Silva BAJ, Nascimento T, Costa LAS, Pereira FV, Machado BA, Gomes GVP, Assis DJ, Druzian JI (2015) Effect of source and interaction with nanocellulose cassava starch, glycerol and the properties of films bionanocomposites. Mater Today Proc 2:200–207

Sofla MRK, Brown RJ, Tsuzuki T, Rainey TJ (2016) A comparison of cellulose nanocrystals and cellulose nanofibres extracted from bagasse using acid and ball milling methods. Adv Nat Sci Nanosci Nanotechnol 7(3):035004. https://doi.org/10.1088/2043-6262/7/3/035004

Souza EE, Vale RS, Vieira JG, Ribeiro SD, Filho GR, Marques FA, Assunção RMN, Meireles CS, Barud HS (2015) Preparation and characterization of regenerated cellulose membranes using cellulose extracted from agroindustrial residues for application in separation processes. Quim Nova 38:202–208

Tan C, Peng J, Lin W, Xing Y, Xu K, Wu J, Chen M (2015) Role of surface modification and mechanical orientation on property enhancement of cellulose nanocrystals/polymer nanocomposites. Eur Polym J 62:186–197

Tasic L, Tsukamoto J, Awan AT, Durán N (2013) Patent: privilege of innovation. Registration number: BR1020130325856, deposit date: 12/18/2013, title: "Process of obtaining bioethanol, spheridine and nanocellulosis from orange bagasse", Registration institution: INPI—Instituto Nacional da Propriedade Industrial

Theivasanthi T, Anne Christma FL, Toyin AJ, Gopinath SCB, Ravichandran R (2018) Synthesis and characterization of cotton fiber-based nanocellulose. Int J Biol Macromol 109:832–836

Thiré RMSM, Andrade CT, Simão RA (2005) Effect of aging on the microstructure of plasticized cornstarch films. Polímeros 15:130–133

Trache D, Hussin MH, Haafiz MM, Thakur VK (2017) Recent progress in cellulose nanocrystals: sources and production. Nanoscale 9:1763–1786

Tsukamoto J, Durán N, Tasic L (2013) Nanocellulose and bioethanol production from orange waste using isolated microorganisms. J Braz Chem Soc 24:1537–1543

Wang LF, Shankar S, Rhim JW (2017) Properties of alginate-based films reinforced with cellulose fibers and cellulose nanowhiskers isolated from mulberry pulp. Food Hydrocoll 63:201–208

Wang Y, Ying Z, Xie W, Wu D (2020) Cellulose nanofibers reinforced biodegradable polyester blends: ternary biocomposites with balanced mechanical properties. Carbohyd Polym 233:115845

Yoo CG, Pu Y, Ragauskas AJ (2017) Ionic liquids: promising green solvents for lignocellulosic biomass utilization. Curr Opin Gr Sustain Chem 5:5–11

Yousefhashemi SM, Khosravani A, Yousefi H (2019) Isolation of lignocellulose nanofiber from recycled old corrugated container and its interaction with cationic starch–nanosilica combination to make paperboard. Cellulose 26:7207–7221

Zain MNF, Yusop SM, Ahmad I (2014) Preparation and characterization of cellulose and nanocellulose from pomelo (Citrus grandis) Albedo. J Nutr Food Sci 5:334. https://doi.org/10.4172/2155-9600.1000334

Zhang Z, O'Hara IM, Doherty WOS (2013) Effects of pH on pretreatment of sugarcane bagasse using aqueous imidazolium ionic liquids. Gr Chem 15:431–438

Zhang Y, Rempel C, Liu Q (2014) Thermoplastic starch processing and characteristics - a review. Crit Rev Food Sci Nutr 54:1353–1370